Electrochemical quartz crystal microgravimetry of poly{pyrrole-co-[3-(pyrrol-1-yl)propanesulfonate]} films: Electrosynthesis, ion transport, and ion assay

3 AUTHORS, INCLUDING:

Subhas Chalasani
East Penn Manufacturing Co

28 PUBLICATIONS **379** CITATIONS

SEE PROFILE

Electrochemical Quartz Crystal Microgravimetry of Poly{pyrrole-co-[3-(pyrrol-1-yl)propanesulfonate]} Films: Electrosynthesis, Ion Transport, and Ion Assay

Sanjay Basak, Chalasani S. C. Bose, and Krishnan Rajeshwar*

Department of Chemistry, Box 19065, The University of Texas at Arlington, Arlington, Texas 76019-0065

The electrosynthesis, ion transport during redox, and ion binding of the title copolymer in aqueous media were studied by electrochemical quartz crystal microgravimetry in conjunction with cyclic voltammetry, coulometry, and ion-selective electrode measurements. Comparisons of the electrochemical behavior of this copolymer with the parent polymer, namely polypyrrole, are also provided. Using the above combination of techniques, quantitative aspects related to the level of oxidation (i.e. "doping") of the electrosynthesized copolymer, the extent of its permselectivity toward cations (K^+) during redox in aqueous chloride electrolytes, and the amount of multiply-charged complex ions [e.g. $Ru(NH_3)_6^{3+}$] that can be bound onto the polymer matrix along with the corresponding thermodynamic partition coefficients of such species are presented.

INTRODUCTION

Electrocatalytic modification of electrode surfaces is now a mature field although examples of functionalized conducting polymers (such as polypyrrole) have only recently begun to proliferate.[1,2] In a previous paper,[3] we demonstrated the capability of the title copolymer (hereafter abbreviated as "PP–PS") to bind multiply-charged complex ions such as Ru-$(NH_3)_6^{3+}$. In this follow-up study, we describe the use of
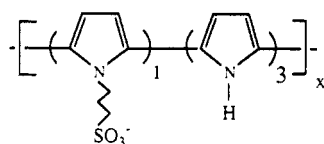
electrochemical quartz crystal microgravimetry (EQCM) for assaying these surface-confined species. We compare these quantitative analyses with the surface coverage obtained via integration of the cyclic voltammetry waves under slow-scan conditions.

The opportunity presented by the use of the EQCM technique also prompted us to explore some aspects related to the electrosynthesis of PP–PS films. Using this technique, we were also able to monitor the ion fluxes during the redox of PP–PS film from the insulating (reduced) to the electronically conductive (oxidized) state. An original impetus for the development of polymers such as PP–PS[4–6] resided with the "self- or auto-" doping ability of the pendant sul-

fonate groups in the copolymer, i.e. the SO_3^- would compensate for the injected positive charge during oxidation of the polymer backbone. Consequently, cations would be ejected from the polymer phase during oxidation of the latter. This contrasts with the behavior of conducting polymers containing *mobile* counteranions (cf. Figure 1). Thus we compare the frequency (mass) vs potential profiles during redox of the two types of polymers. We show that the extent of permselectivity of PP–PS (toward cations) is sensitive to the nature of the co-ions associated with the sulfonate groups. At relatively high levels of oxidation and when the copolymer is loaded with Ru-$(NH_3)_6^{3+}$, anion movement is observed on oxidative "doping" of the polymer.

EXPERIMENTAL SECTION

Chemicals. Pyrrole and 1,3-propanesultone (*CAUTION*: 1,3-propanesultone is a suspected carcinogen) were from Aldrich and $Ru(NH_3)_6Cl_3$ was from Strem Chemicals (ACS reagent grade). 3-(Pyrrol-1-yl)propanesulfonate (hereafter abbreviated as "pyrrole sulfonate") was synthesized by reacting pyrrole potassium salt with 1,3-propanesultone.[4a] Pyrrole was purified by passage through a Pasteur pipette microcolumn containing glass wool and activated Al_2O_3. Double-distilled water was from a Corning Megapure system. All experiments were performed on carefully deaerated solutions and under a nitrogen blanket.

Instrumentation and Accessories. The EQCM apparatus has been described elsewhere.[7] An AT-cut quartz resonator (5 MHz) from Valpey-Fisher with Au deposited on either side was used for mass sensing and as a working electrode for electrochemistry. This was clamped via an O-ring seal such that the area exposed to the solution (0.7 cm²) was less than the oscillation area. An Ag/AgCl/3 M KCl electrode (Bioanalytical Systems) was used as reference; all the potentials are quoted with respect to this reference. A large Pt foil was used as the counterelectrode in all cases. The potassium ion fluxes were monitored (in the solution adjacent to the working electrode) with an ion-selective electrode (ISE) (Model MI-442 from Microelectrodes Inc., Londonberry, NH) using an Orion Research Model 501 digital ion analyzer.

Procedures. The PP–PS films were potentiostatically deposited at +850 mV onto the Au surface of the quartz crystal from aqueous solutions containing 50 mM pyrrole and 25 mM pyrrole sulfonate using 150 mC of anodic charge. It must be pointed out that *no* supporting electrolyte was used during polymer growth.[3] For the scanning experiments, the films thus freshly synthesized were "exercised" in 0.2 M KCl by cycling between –900 and +300 mV for ~20 min. During this procedure, the films steadily increased in mass until equilibrium was attained as signaled by a saturation in the film mass (cf. Figure 3b). We suppose that this is partly a consequence of the swelling of the film as noted by previous authors for other types of redox polymer films.[8,9] (Also see below.) The exercised films were then scanned

* Author for correspondence.
(1) Deronzier, A.; Moutet, J.-C. *Acc. Chem. Res.* **1989**, *22*, 249–255.
(2) Curran, D.; Grimshaw, J.; Perera, S. *Chem. Soc. Rev.* **1991**, *20*, 391–404.
(3) Basak, S.; Rajeshwar, K.; Kaneko, M. *Anal. Chem.* **1990**, *62*, 1407–1413.
(4) (a) Sundaresan, N.; Basak, S.; Pomerantz, M.; Reynolds, J. R. *J. Chem. Soc., Chem. Commun.* **1987**, 621–622. (b) Reynolds, J. R.; Sundaresan, N.; Pomerantz, M.; Basak, S.; Baker, C. K. *J. Electroanal. Chem. Interfacial Electrochem.* **1988**, *250*, 355–371.

(5) Bidan, G.; Ehui, B.; Lapkowski, M. *J. Phys. D: Appl. Phys.* **1988**, *21*, 1043–1054.
(6) Zhong, C.; Storck, W.; Doblhofer, K. *Ber. Bunsenges. Phys. Chem.* **1990**, *94*, 1149–1155.
(7) Bose, C. S. C.; Rajeshwar, K. *J. Electroanal. Chem. Interfacial Electrochem.*, in press.
(8) Schroeder, A. H.; Kaufman, F. B. *J. Electroanal. Chem. Interfacial Electrochem.* **1980**, *113*, 209–224.
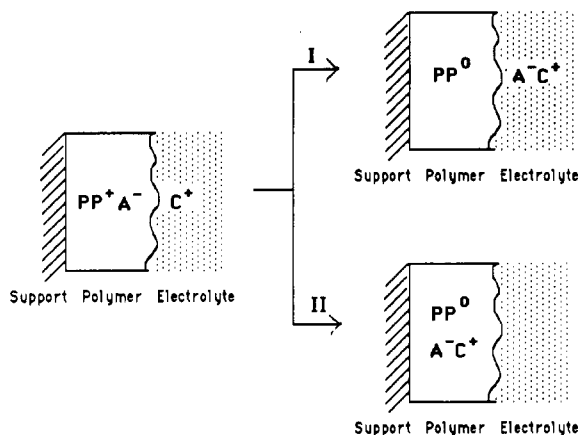
Figure 1. Highly schematized model for the anion (I) and cation (II) transport pathway during redox of a supported polypyrrole (PP) electrode.
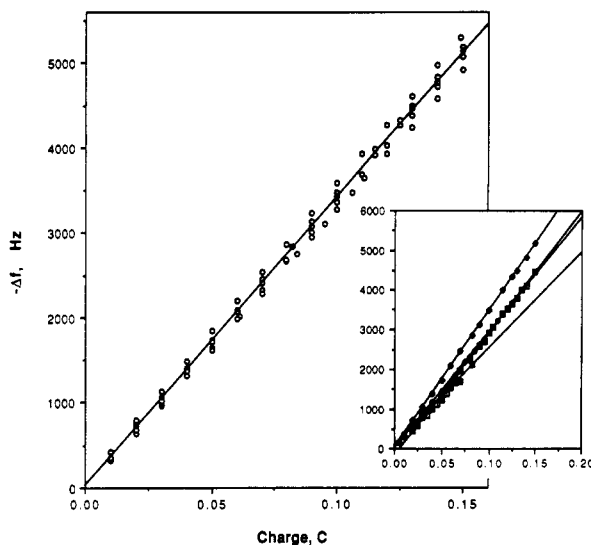

Figure 2. Combined EQCM–coulometry data shown as $-\Delta f$ vs charge plots for the electrosynthesis of a PP–PS copolymer under conditions described in the text. Five replicate runs on a fresh solution are shown in the main figure. The inset shows the effect of solution storage or aging, the lines with decreasing slopes corresponding to 0, 2, 6, and 7 days, respectively. The lines are least-squares fits of the data.

between $\sim$−900 and +300 mV either at 5 or 50 mV/s for the various EQCM–coulometry experiments described below. (Exceptions are the data in Figure 3, where the initial equilibration behavior is also considered.)

For loading of the PP–PS films with $Ru(NH_3)_6^{3+}$, freshly prepared and exercised samples (150 mC anodic growth charge corresponding to $\sim$0.5-μm film thickness, cf. ref 3) were cycled (nominally at 50 mV/s) between +300 and −900 mV in 0.2 M KCl containing the requisite amount (2, 4, or 6 mM) of $Ru(NH_3)_6Cl_3$. For the potential-step and the potassium ISE measurements, thicker PP–PS films (either $\sim$1.3 or $\sim$2.5 μm) were employed to enhance the measurement sensitivity.

RESULTS AND DISCUSSION

Electrosynthesis of PP–PS on Au. Figure 2 contains EQCM–coulometry data for the electrosynthesis of PP–PS films on Au from a solution containing pyrrole and pyrrole sulfonate. These data are shown in the form of a $-\Delta f$ vs charge plot, wherein $-\Delta f$ is the frequency decrease of the quartz resonator corresponding to its mass loading (i.e. the Sauerbrey correlation, cf. ref 10). The data in the main figure correspond to five replicate runs performed on different days,

each time with a *fresh* solution. Faraday's law yields

$$Q = \frac{nF\Delta m}{M} \quad (1)$$

In eq 1, Q is the (anodic) charge consumed in the polymerization reaction, n is the electron stoichiometry, F is the Faraday constant (96 487 C/mol), Δm is the mass deposited, and M its molar mass. The slope of the plot in Figure 2 corresponds to 34 428 Hz/C. This, in turn, translates to 34 428 × 13 ng/C based on our calibration of the EQCM system.[7] The formula of the repeating unit in our PP–PS copolymer (as determined by elemental analyses on samples synthesized under the conditions employed in this study) (see structure shown above) yields a value for M of 95.5 g/mol.

The above information permits the computation of n in eq 1. We obtain a value of 2.21 in good agreement with that (2.25) expected from the elemental analyses.[3] Thus one unit of positive charge is delocalized over four pyrrole rings in the oxidized PP–PS copolymer, which consumes 2.25 e^-/mol during growth, i.e. 2 e^- for the ring coupling step and the residual charge for the doping of the polymer. The good agreement between the two sets of values supports the notion that the polymerization essentially proceeds with $\sim$100% coulombic efficiency.

The inset in Figure 2 illustrates that "aged" solutions yield much lower slopes (the slopes in Figure 2 correspond to M/nF), and thus higher "effective" n values. The meaning of this trend is that the polymerization occurs with efficiencies lower than 100%. The data in the inset were acquired on solutions of pyrrole and pyrrole sulfonate which had been stored (in a refrigerator) over a period of $\sim$7 days. It must be noted that these growth media did not show any visible darkening (associated for example with the degradation of pyrrole) and yet were obviously less than optimal. Thus these data are presented with a view to underline the care that must be exercised with the polymer electrosynthesis procedure. On the other hand, highly reproducible results can indeed be obtained with the use of fresh solutions for the film growth. We note that similar trends have been reported by previous authors[11] for polypyrrole.

Ion Transport during the Redox of PP–PS Films. Figure 3 contains a comparison of concurrent EQCM–cyclic voltammetry (CV) profiles for polypyrrole (Figure 3a) and PP–PS (Figure 3b). These experiments were performed in 0.2 M KCl at a potential scan rate of 50 mV/s. We have discussed in detail the behavior of polypyrrole in this medium elsewhere.[12] Briefly, the CV scans on repetitive cycling of a freshly grown film show the usual (broad) redox waves associated with the switch of the polymer between the insulating and conductive states. Correspondingly, the frequency (mass)–potential EQCM scan shows a mass increase due to the anion uptake on oxidation of the polymer. (Nonetheless, this material strictly is *not* permselective to chloride as discussed elsewhere, ref 12.) Equilibration of the polymer in the KCl electrolyte is facile, as shown by the rapid saturation of the CV charge envelope and the EQCM frequency; this is a point we have also asserted in the previous study.[12]

On the other hand, the corresponding data for the PP–PS copolymer reveal two interesting differences relative to the parent polymer. First, the frequency (mass) change is opposite in sense (to the polypyrrole case) as the electrode is scanned between −900 and +300 mV, i.e. the mass *decreases* on oxidation of the polymer. Second, the first cycle both in CV and in EQCM is markedly different from the successive

(9) Inzelt, G.; Horányi, G. *J. Electrochem. Soc.* **1989**, *136*, 1747–1752.
(10) Sauerbrey, G. *Z. Phys.* **1959**, *155*, 206–222.

(11) Scharifker, B. R.; Garcia-Pastoriza, E.; Marino, W. *J. Electroanal. Chem. Interfacial Electrochem.* **1991**, *300*, 85–98.
(12) Bose, C. S. C.; Basak, S.; Rajeshwar, K., submitted for publication.
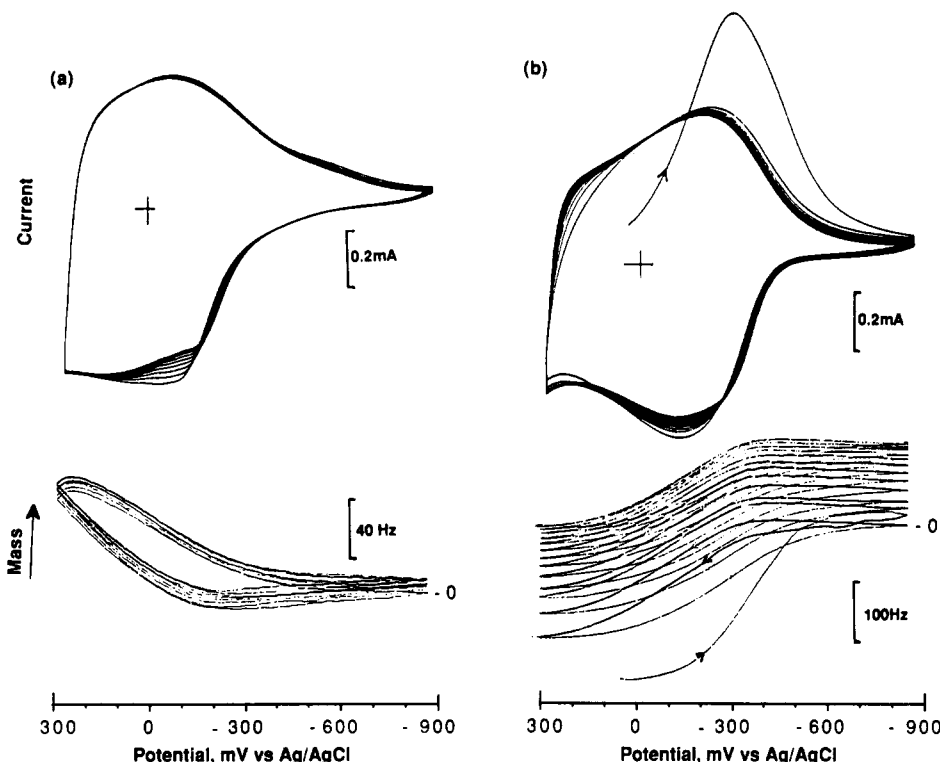
Figure 3. Cyclic voltammetry (top) and EQCM (bottom) profiles on repetitive cycling at 50 mV/s of freshly grown polypyrrole (Figure 3a) and PP–PS (Figure 3b) films in 0.2 M KCl. The films were ~0.5 μm thick in both cases.
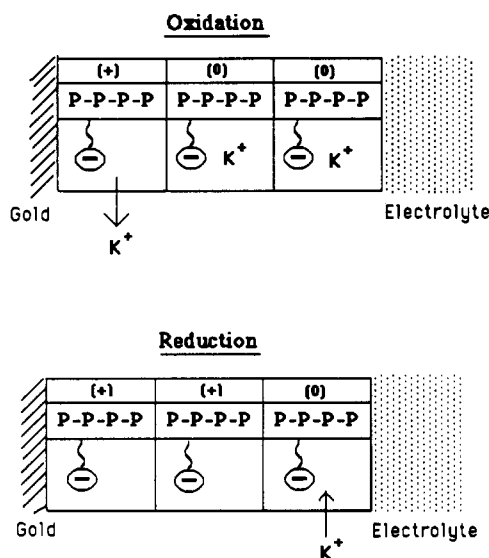

Figure 4. Highly schematized model of the "auto- or self-" doping characteristic of pendent SO_3^- groups in the PP–PS copolymer. Refer to the text for details.

scans as the polymer is first reduced by scanning to the negative potential limit (Figure 3b).

We will show below that the mass loss is due to the ejection of the K^+ ions from the polymer as positive charge is injected into its backbone, i.e. the SO_3^- groups now manifest their autodoping characteristics (Figure 4). The scheme shown in Figure 4 also takes into account the zone movement, i.e. the oxidation proceeds from the support electrode/film interface outward, while the reduction process involves the movement of the insulating zone inward from the film/electrolyte interface. This model is derived from that proposed and verified by Aoki et al.[13] for the polypyrrole parent polymer.

Complications not taken into account in the simple scheme in Figure 4 are neutral salt and anion transport effects (see below).

"First cycle" effects of the sort seen in Figure 3b have been discussed by previous authors for polypyrrole containing other anionic dopants.[14,15] We have also observed such behavior[16] for polypyrrole doped with pyrene- or naphthalenesulfonate. The difference in the equilibration behavior between the two types of polymers in Figure 3 underlines their chemical dissimilarity. Aside from solvent swelling, neutral salt (i.e. KCl) uptake by PP–PS could also contribute to its slow equilibration. Further (quantitative) experiments on PP–PS, including those related to $Ru(NH_3)_6^{3+}$ binding which are discussed in what follows, were performed on films equilibrated as in Figure 3b.

Figure 5a contains representative data from EQCM–coulometry experiments on an exercised PP–PS film which was subsequently scanned (between –900 and +300 mV at 5 mV/s) in 0.2 M KCl. The dashed line in Figure 5a shows the behavior expected for the permselective (potassium ion transport) case (cf. Figure 4). There is good agreement with the cation transport model especially at the negative potentials within the scan range (or equivalently small values of the redox charge). As increasing amounts of positive charge are injected into the polymer backbone, deviation from permselectivity sets in.

A further comparison with polypyrrole in this regard reveals an intriguing symmetry. Thus polypyrrole manifests cation transport at more negative potentials followed by the (dominant) anion injection pathway at higher levels of oxidation of the polymer.[12] A mirror-image trend applies to PP–PS. Thus the (major) cation transport pathway in this latter case is seen at low levels of polymer oxidation, followed by the anion component at more positive potentials.

(13) (a) Aoki, K. *J. Electroanal. Chem. Interfacial Electrochem.* 1990, *292*, 53–62. (b) Tezuka, Y.; Aoki, K. *Ibid.* 1989, *273*, 161–168.
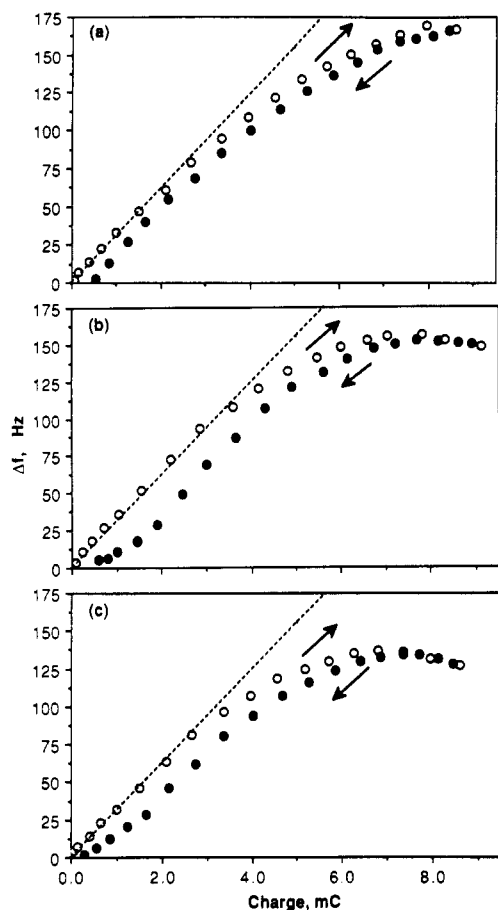
(14) Wernet, W.; Wegner, G. *Makromol. Chem.* 1987, *188*, 1465–1475.
(15) Beck, F.; Braun, P.; Schloten, F. *J. Electroanal. Chem. Interfacial Electrochem.* 1989, *267*, 141–148.
(16) Krishna, V.; Ho, Y.-H.; Basak, S.; Rajeshwar, K. *J. Am. Chem. Soc.* 1991, *113*, 3325–3333.

Figure 5. Combined EQCM-coulometry data shown as Δf-charge plots of a well-exercised PP-PS copolymer film (cf. Experimental Section) before and after binding of $Ru(NH_3)_6{}^{3+}$ (parts b and c correspond to solution $Ru(NH_3)_6{}^{3+}$ levels of 4 and 6 mM, respectively). These data were acquired in 0.2 M KCl with potential cycling at 5 mV/s between −900 and +300 mV. The (○, ●) symbols pertain to the two scan directions. The dashed lines in each frame are those expected for permselective potassium ion transport.

Table I. Analyses of K^+ Transport during Redox of Three Au-Supported PP-PS Copolymer Films in 0.05 M LiCl

run no.	Q_{ox},[a] mC	$[K^+]$,[b] 10^5 mol/L	Q_K,[c] mC	Q_K/Q_{ox}[d]
1	11.5	6.4	12.4	1.08
2	13.0	6.8	13.1	1.01
3	9.7	5.1	9.8	1.01

[a] Charge consumed in the 0 mV ↔ −500 mV potential step. [b] Concentrations refer to the electrolyte phase and were measured by a potassium ISE. [c] The corresponding charge was computed from the values in the third column using Faraday's law. [d] "Ideal" permselectivity should yield a value of unity.

The behavior in the cation transport potential regime (0 ↔ −500 mV) was probed in more detail for PP-PS by potassium ISE and potential step measurements. To this end, a ~1.3-μm PP-PS film was repetitively stepped in potential in 0.2 M KCl between 0 and −500 mV with a dwell time of ~3 min at each potential. The corresponding charge was monitored. The PP-PS film was then disconnected at −500 mV and removed from the solution in the reduced state. After thorough washing, the film was transferred to 0.05 M LiCl in the EQCM cell (solution volume: 2 mL). A potential of 0 mV was now applied for 3 min; concomitantly, the K^+ ion release from the film was monitored with an ISE. The results are tabulated in Table I. Replicate runs on three different samples are presented to illustrate the sort of variability from film to film. These data obviously are in

Table II. Experiments Similar to Those in Table I but for Thicker (~2.5 μm) PP-PS Films Supported on a Pt Foil[a]

run no.	Q_{ox}, mC	$[K^+]$, 10^5 mol/L	Q_K, mC	Q_K/Q_{ox}
1	36.0	19.0	36.6	1.02
2	35.5	12.0	34.7	0.98
3	26.0	13.0	25.1	0.97

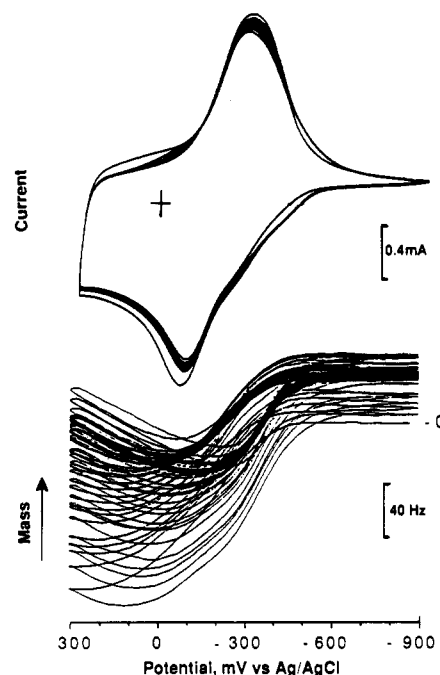[a] The 0.05 M LiCl solution volume was 2.0 mL in entries 1 and 3 and 3.0 mL in entry 2.

Figure 6. Cyclic voltammetry (top) and EQCM (bottom) profiles of a PP-PS copolymer film (similar to that in Figure 3) in 0.2 M KCl containing 6 mM $Ru(NH_3)_6Cl_3$. Other conditions are in Figure 3.

good accord with the permselectivity of PP-PS toward K^+ under these conditions.

Table II contains further confirmation of this trend from ex situ coulometry-ISE measurements on a thicker (~2.5 μm) PP-PS film which was supported on a 1.76-cm^2 Pt foil.

We attribute the deviation from permselectivity of PP-PS at more positive (> ~0 mV) potentials to the onset of Cl$^-$ ion transport. Thus while the positive charge in the polymer backbone is balanced by the $SO_3{}^-$ groups at the incipient stages of doping, further neutralization of this charge necessarily is accompanied by chloride ion ingress into the polymer from the electrolyte. This sequence is not unlike that which has been discussed by other authors, both for PP-PS[6] as well as for polypyrrole containing large anions such as dodecyl sulfate[17] and poly(styrenesulfonate).[18]

However, one interesting aspect of the anion transport regime as revealed by this study, is that this process is sensitive to the nature of the co-ions associated with the $SO_3{}^-$ groups. Thus, $Ru(NH_3)_6{}^{3+}$ ions have a marked influence in this potential regime, as discussed next.

Binding of $Ru(NH_3)_6{}^{3+}$ by PP-PS. Figure 6 contains CV and EQCM data that reflect the $Ru(NH_3)_6{}^{3+}$ uptake by a ~0.5-μm PP-PS film. This film was cycled at 50 mV/s in a 6 mM solution of the complex ion in 0.2 M KCl. The CV profile clearly is different from the virgin electrolyte case (Figure 3b) and is similar to those observed in our previous study.[3] The frequency (mass) vs potential profiles also are

(17) Zhong, C.; Doblhofer, K. Electrochim. Acta 1990, 35, 1971–1976.
(18) Lien, M.; Smyrl, W. H.; Morita, M. J. Electroanal. Chem. Interfacial Electrochem. 1991, 309, 333–340.

Table III. EQCM and Voltammetric Assay of $Ru(NH_3)_6^{3+}$ Bound in ~0.5-μm PP–PS Copolymer Films[a]

C_{soln}^{Ru}, mM	$-\Delta f$,[b] Hz	Q_{Ru},[c] mC	surface coverage, Γ_{Ru}, 10^9 mol cm^{-2}		C_{poly}^{Ru},[d] mM	K_D[e]
			EQCM	voltammetry		
2	20	0.25	4.4	3.7	88 (74)	44 (37)
4	40	0.40	8.8	5.9	176 (118)	44 (30)
6	50	1.00	11.0	14.8	220 (296)	37 (49)

[a] Values averaged from replicate (at least two) analyses on identically prepared samples and are reproducible within ±10%. [b] The saturation frequency change as measured by EQCM at –900 mV (cf. Figure 6). [c] Charge encompassed in a slow-scan CV wave (cf. Figure 7). [d] Computed using the EQCM assay in column 4 and 0.5-μm film thickness. The values in parentheses are determined by CV using the data in column 5. [e] The values shown are those determined by EQCM; those in parentheses are determined by CV.
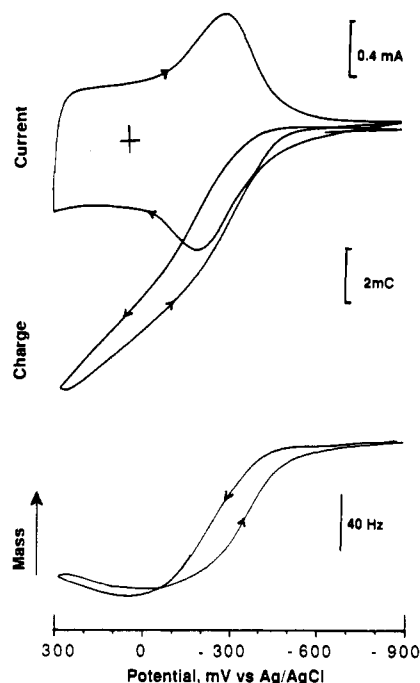

Figure 7. Data for the sample as in Figure 6 after $Ru(NH_3)_6^{3+}$ loading but now scanned at 5 mV/s in 0.2 M KCl. The charge–potential scan is also additionally included.

markedly altered when the complex ion is present. Particularly noteworthy is the "upturn" in the mass vs potential scans at potentials positive of 0 mV (compare with Figure 3b). On the other hand, the frequency change at –900 mV of this *pre-equilibrated* PP–PS film reflects the $Ru(NH_3)_6^{3+}$ "irreversibly" loaded onto the polymer film. We will return to this later when we discuss the ion assay.

Transfer, after thorough washing of the $Ru(NH_3)_6^{3+}$-loaded PP–PS copolymer, followed by cycling in *neat* 0.2 M KCl yield the CV, coulometry, and EQCM data shown in Figure 7. Note that the CV profile now collapses to that diagnostic of surface-confined redox species (i.e. zero peak separation, no diffusion tail) as discussed by us previously.[3] The mass vs potential profile also is different from that contained in both Figures 3b and 6 in that the upturn is unmistakable (albeit much reduced from that in Figure 6) relative to Figure 3b and the hysteresis is more pronounced in Figure 7.

The transport model in Figure 8 satisfactorily accounts for all the trends seen in Figures 6 and 7. This scheme is shown for a 12-ring system (corresponding to three units of positive charge in the copolymer backbone, see above). For brevity's sake, the zone juxtaposition during redox is *not* specified in Figure 8 (unlike in the model in Figure 4). The model in Figure 8 features two types of $Ru(NH_3)_6^{3+}$ binding—the weakly-bound (reversible) species accounting for the "upturn" in the mass–potential scans in Figure 6. (Recall that the "heavy" $Ru(NH_3)_6^{3+}$, $M = 203$ g/mol, effectively swamps the other species undergoing flux during polymer redox). The

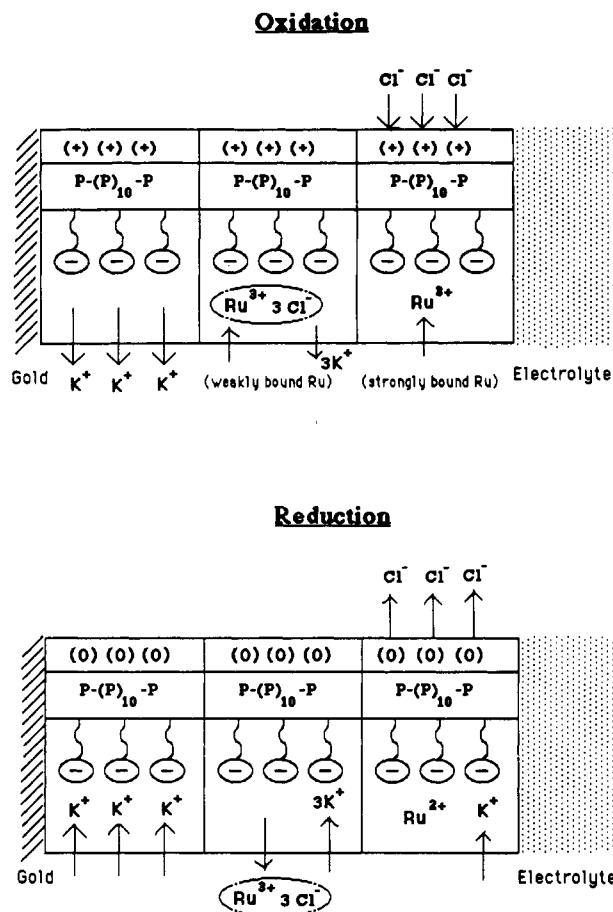**Figure 8.** Highly-schematized model for the ion fluxes during redox of a $Ru(NH_3)_6^{3+}$-loaded PP–PS copolymer. Refer to the text for details.

weaker upturn clearly seen in Figure 7 is attributed to Cl$^-$ ingress into the PP–PS copolymer during its oxidation.

Interestingly enough, the extent of this anion flux, and thus the departure from strict K$^+$ ion permselectivity, appears to scale with the complex ion content of the copolymer as the data in Figure 5 parts b and c, illustrate.

The change in frequency at the negative extremity of the potential excursion, e.g. –900 mV, as mentioned previously, affords an estimate of the $Ru(NH_3)_6^{3+}$ irreversibly bound onto the copolymer film. Table III contains the "surface excess" Γ_{Ru} (mol cm^{-2}) of the complex ion thus determined as a function of the solution concentration. Also shown in the table are estimates of Γ_{Ru} from integration of the slow-scan CV charge.[19] The two types of assays are in reasonable agreement with one another. Also shown in Table III are the values of the partition coefficient, K_D for $Ru(NH_3)_6^{3+}$ in PP–PS from KCl as determined by the two techniques. These

(19) Murray, R. W. In *Electroanalytical Chemistry*; Bard, A. J., Ed.; Marcel Dekker: New York, 1983; pp 191–368.

values are in good agreement with those reported by us earlier using CV.[3]

In conclusion, we have built upon the previous study[3] to further explore aspects related to the electrosynthesis, ion transport, and ion binding of the PP–PS copolymer. We have been able to show via a combination of several electrochemical techniques that this copolymer is permselective to cations (K^+ ions in this particular study) at low levels of oxidation. Anion transport sets in at higher doping levels. The copolymer also becomes less permselective in the presence of bound multiply-charged complex ions. The bound ion assay and partition coefficients obtained via the EQCM technique are in reasonable agreement with values obtained in the previous study.[3] From an analytical perspective, we believe that the results presented above further illustrate the utility of EQCM for the study of chemically modified electrode surfaces.

ACKNOWLEDGMENT

Registry No. Ru, 7440-18-8; K, 7440-09-7; pyrrole/3–(pyrrol-1-yl)propanesulfonate (copolymer), 122350-18-9.